THE ANNALS OF "DUNAREA DE JOS" UNIVERSITY OF GALATI
FASCICLE III, 2009, Vol.32, No.1, ISSN 1221-454X
ELECTROTECHNICS, ELECTRONICS, AUTOMATIC CONTROL, INFORMATICS

ACTIVE POWER FILTER WITH INDIRECT CONTROL FOR LINE-FREQUENCY CONTROLLED RECTIFIERS

E. Rosu, M. Culea, T. Dumitriu, T. Munteanu and R. Paduraru

"Dunarea de Jos" University, Galati, Romania
Emil.Rosu@ugal.ro

Abstract: Line-frequency controlled rectifiers have two major disadvantages: variable displacement power factor and high harmonic current fed to the power supply. If the power converter is large, e.g. for rolling mills drives, it is necessary to use a local reactive-power and harmonics compensation The control of shunt active power filters, APF, using PWM inverters, consists in generating a reference by separating, using different methods, the harmonics to be eliminated. The methods used are time-consuming and need dedicated control and signal processing equipments. To avoid these setbacks a new method is proposed in the paper. The active power filter is a current PWM rectifier with voltage output and a capacitor on the DC side. The PWM rectifier is controlled so that the sum of its current and the non-linear load's current is a sinusoid in phase with network voltage. The control block schema as well as simulation results are presented.

Keywords: Active Power Filters, PWM Rectifiers, Hysteresis Control, Line-frequency Controlled Converter, THD.

1. INTRODUCTION

Line-frequency controlled converter, LFCC, draws from alternative supply a considerable current harmonics and reactive power (Mohan, 2000). In a 6-pulse converter, Fig.1, the most common line-frequency controlled converter, the drawn a.c. current contains the characteristic harmonics of the order $6k \pm 1$, and harmonics amplitudes are variable, depending of the firing angle and load.
On the other hand the converter draws reactive power from the mains both in rectifier and inverter regime. The displacement power factor has an approximate value

$$(1)\ \cos\varphi = \cos(\alpha + \frac{u}{2})$$

where α is the firing angle and u is the commutation interval (Rahmani, 2003). The mains voltage and

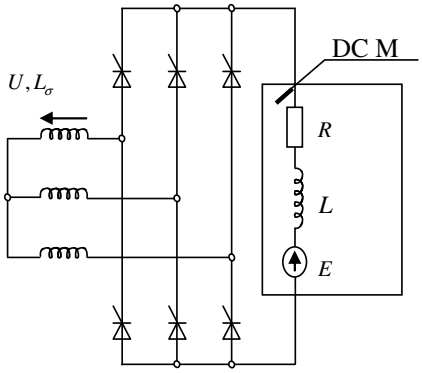

Fig.1. Line-frequency controlled converter.

current waveforms, of a controlled rectifier are presented in Fig.2 for a firing angle $\alpha = 20^\circ$ and a load current $I_d = 36A$, the load being a DC motor with the following parameters: $R = 1\Omega$, $L = 10mH$ and rated voltage $U_N = 220V$. The THD

This paper was recommended for publication by Ion Bivol

coefficient of the drawn current is 31.50%, while $\cos\varphi = 0.902$. These results indicate the necessity of APF using to compensate the harmonic and reactive current components.

The classical structure of a three-phase APF realised using a voltage inverter is presented in Fig. 3, where SD is the non-linear load. The APF injects a phase current $i_F(t)$ so that the total phase current drawn from the mains,

$$(2) \quad i_R(t) = i_S(t) - i_F(t),$$

is sinusoidal and the voltage and current phases are identical.

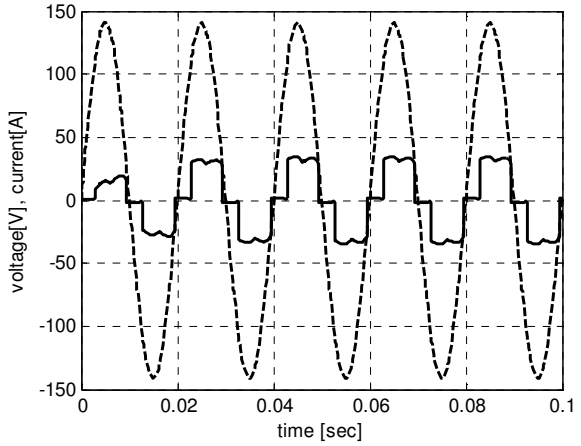

Fig.2. Supply voltage and drawn current.

The APF's phase current is

$$(3) \quad i_F(t) = \tilde{i}_S(t) + i_F^1(t)$$

where the polluting component

$$(4) \quad \tilde{i}_S(t) = i_{SK}(t) + i_{SQ}(t)$$

$i_{SK}(t)$ being the sum of higher order harmonics, $i_{SQ}(t)$ the drawn reactive current, and $i_F^1(t)$ is the fundamental current used to keep the capacitor C charged.

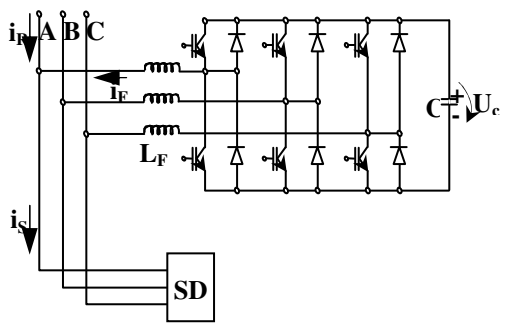

Fig.3. The classical APF structure.

Generating a current i_F through L_F inductor means the control of the APF with a reference given by equation

$$(5) \quad i_F^*(t) = i_{SK}^*(t) + i_{SQ}^*(t) + i_F^{1*}(t) \ .$$

Separation of higher order harmonics and reactive current components from the fundamental is a rather complicated procedure. On the other hand the component $i_F^1(t)$ can be easily calculated by taken into consideration the level and ripple of the capacitor C voltage. In (El-Habrouk, 2000; Rahmani, 2003) several methods concerning the higher harmonics and reactive components separation are presented, such as instantaneous power method or components filtering. Several other methods are presented in literature but they are usually application oriented.

2. INDIRECT APF TOPOLOGY

A new approach, called indirect control, proposed in (Rosu, 2006), is developed in this paper for a LFCC. The application does not need a prior knowledge of the non-linear load's current spectrum and reactive component.

The schematic of the system is presented in Fig.4. The transformer leakage inductance can be neglected because

$$(6) \quad L_\sigma \ll L_K \ ,$$

and, for the beginning, the inductances L_F will not take into consideration. Unlike the classical structure, the supply of the load and APF is done through the inductor L_K in a structure specific to PWM current rectifiers with voltage output.

The phase current drawn from the mains is

$$(7) \quad i_{RA}(t) = i_{SA}(t) + i_{FA}(t) .$$

The non-linear load's phase current is

$$(8) \quad i_{SA}(t) = i_{SA}^1(t) + i_{SAK}(t) + i_{SAQ}(t)$$

where $i_{SA}^1(t)$ is the fundamental active current component, $i_{SAK}(t)$ the sum of higher order harmonics, and $i_{SAQ}(t)$ the reactive current component. On the other hand APF current will be of the form

$$(9) \quad i_{FA}(t) = i_{FA}^1(t) + \tilde{i}_{FA}(t) \ ,$$

where $i_{FA}^1(t)$ has the same signification as $i_F^1(t)$, and $\tilde{i}_{FA}(t)$ an unspecified non-sinusoidal current component. The L_K inductor, which is required to limit the gradient of the APF current, is cross by total drawn current $i_{RA}(t)$. This current must be sinusoidal and must have the same phase as mains voltage. The

APF is controlled so the sum

$$(10)\quad \tilde{i}_{FA}(t)+i_{SAK}(t)+i_{SAQ}(t)=i_{SIN}\,,$$

where i_{SIN} is a sinusoidal current at the point of common coupling in phase with the voltage. This is possible because the APF current $i_{FA}(t)$ is part of the drawn current $i_{RA}(t)$. On the other hand the APF reference, given by equation (5), will be indirectly generated, the drawn current $i_{RA}(t)$ being the controlled current.

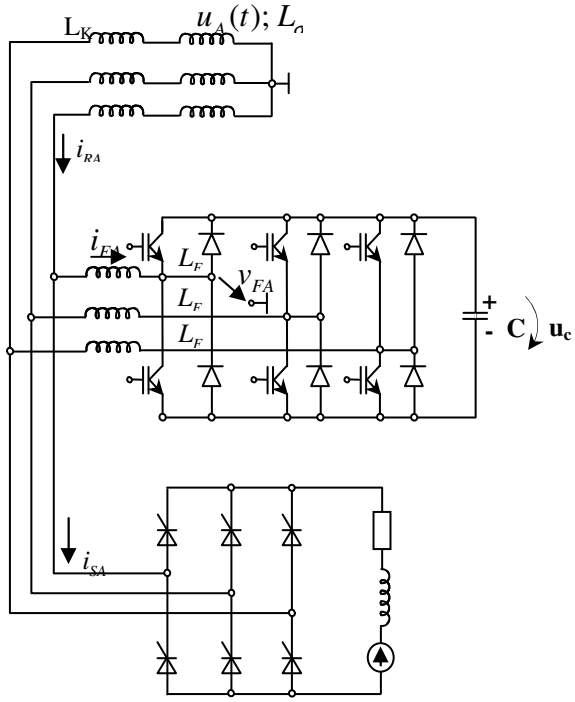

Fig.4. The indirect APF topology.

There are two different working regimes. For the first, the non-linear load disconnected, it can be shown that

$$(11)\quad L_K\frac{di_{RA}}{dt}=u_A(t)-v_{FA}(t)$$

where

$$(12)\quad u_A(t)=U_A\sqrt{2}\sin\omega t$$

is the phase mains voltage,

$$(13)\quad i_{RA}(t)=i_{FA}(t)=i^1_{FA}(t)$$

the drawn current, and $v_{FA}(t)$ the input APF voltage. The equation (11) can be rewritten as

$$(14)\quad \frac{di_{RA}}{dt}=\frac{u_A(t)-v_{FA}(t)}{L_K}\,.$$

The supply voltage U_A is constant, while r.m.s. of v_{FA} has the value

$$(15)\quad V_F=\sigma U_C\,,$$

where σ is the amplitude modulation index. The voltage U_C is bigger than line-commuted rectifier output due to boost characteristic of the PWM rectifiers. From (14) and (15) results that the derivative of the current $i_{RA}(t)$ is determined by the inductor L_K and input APF voltage. If the derivate is constant, then the current ripple and switching APF frequency will be constant. To obtain this desideratum the capacitor voltage U_C must be controlled at the imposed value given by equation (15). On the other hand a smaller L_K increase performances of the filter, but with a bigger derivative of the current. For this working regime the drawn current, given by equation (13), has a small value and it is not concluded for the calculus of the inductor L_K.

In the second working regime, non-linear load connected, the drawn current is given by, equations (7), (8) and (9),

(16)
$$i_{RA}(t)=i^1_{SA}(t)+i_{SAK}(t)+i_{SAQ}(t)+i^1_{FA}(t)+\tilde{i}_{FA}(t)\,,$$

the current being consistent and variable. Equation (14) can be used to calculate the inductor L_K, taken into consideration the maximum admissible current gradient and imposed voltage U_C. The capacitor C can be calculated base on the energy variation which occurs in the d.c. circuit and an imposed voltage ripple.

The inductors L_F are necessary in order to assure the working conditions of the LFCC. Periodically the APF produces input short-circuits, i.e.

$$(17)\quad v_{FA}(t)=0\,.$$

On the other hand without L_F the line voltages v_{FA}, v_{FB}, v_{FC} are the input voltages for the LFCC. Zero value of the input voltages are due to the following influences:

- If the control, e.g. the firing angle, is applied while input voltage is zero, the controlled thyristor does not start the conduction, the working becomes asymmetrical and the output voltage diminishes;
- Obviously the annul of the input voltages could produced discontinuous current with well-known effects;
- APF switching frequency will appear in the waveform of LFCC output voltage;
- The LFCC output voltage will be bigger than normal since the APF has a boost characteristic.

To diminish these effects and to assure the continuous output current the inductors L_F are placed between

LFCC and APF, having the value

$$L_F < 0.1L_K \quad (18)$$

3. CONTROL STRATEGIES

Different control strategies, such as open-loop sinusoidal PWM, open or closed loop hysteresis control can be used. In the paper is developed the closed loop hysteresis control since a current must be controlled.

From (14) it can be observed that the capacitor voltage U_C the drawn current has to be determined.

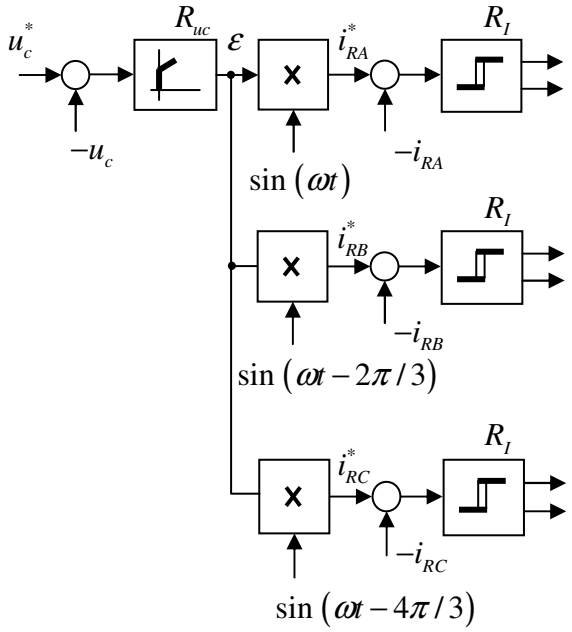

Fig.5. The APF control strategy.

The choice of U_C as a controlled value, via R_{UC} PI controller, Fig.5., was presented above in the paper. The error ε of the realisation of the capacitor voltage is transformed into a reference for the input phase currents in the following manner

$$\begin{aligned} i_{RA}^* &= \varepsilon.\sin(\omega t) \\ i_{RB}^* &= \varepsilon.\sin(\omega t - 2\pi/3) \\ i_{RC}^* &= \varepsilon.\sin(\omega t - 4\pi/3) \end{aligned} \quad (19)$$

which have the same phase as the mains voltage. The current is controlled using a hysteresis controller R_I with an acceptable hysteresis band relating to the current ripple and switching frequency.

4. SIMULATION RESULTS

To validate the proposed control scheme and indirect APF properties the model presented in Fig. 4 and 5 was used.

The parameters of the schema are:

- Supply: phase voltage 100V, 50 Hz, $L_\sigma = 0$;
- APF: $C = 1000\mu F, U_C = 360V, L_K = 1.5mH$, $L_F = 0.1mH$;
  Hysteresis band 1 A.
- LFCC and D.C. motor, $U_N = 220V, R = 1\Omega$, $L = 20mH$.

In Fig.6 the waveforms of the phase voltage and drawn current, for a non-simultaneously APF and LFCC connection, are presented. The first, when $t = 0$, APF is connected. After a very short time, about one period, the dynamic regime is finished, the capacitor is charged and U_c is 360 V, Fig. 7, while the drawn current, which has a small value, becomes sinusoidal. There are two drawbacks. At the beginning the drawn current has a great value, more than 50A, being necessary its limitation which can be achieved by conventional methods. Also the capacitor voltage overshoot, Fig. 7, of around 20%, could be unacceptable.

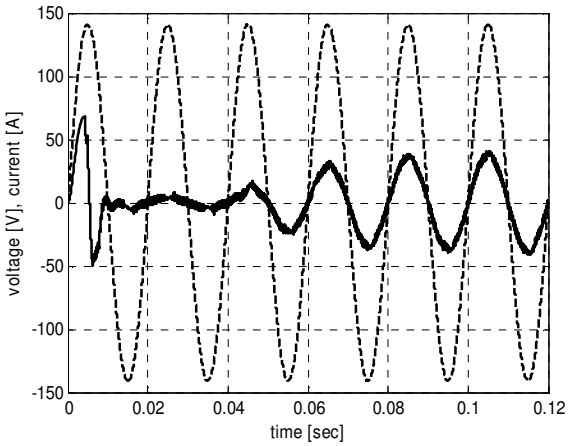

Fig.6. Phase voltage and current for rectifier mode, $\alpha = 20^\circ$.

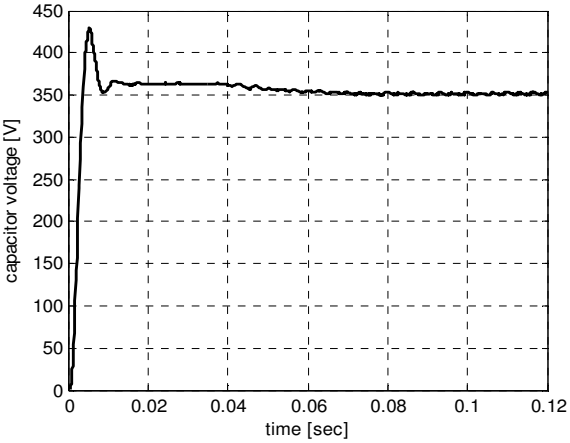

Fig. 7. The waveform of the capacitor voltage U_C.

The LFCC is connected at time $t = 0.04$ sec in the rectifier mode at a firing angle $\alpha = 20^\circ$. In Fig.8 the

variation of the load current is plotted. The current rising is strongly influenced by the electric time constant of the DC motor

$$(20)\quad \tau = \frac{L}{R} = 10 m\sec .$$

On the other hand the drawn current, Fig.6, give a sinusoidal form after one period and it continues to rise accordingly with load current. At the end of the dynamic regime THD is 6.6%.

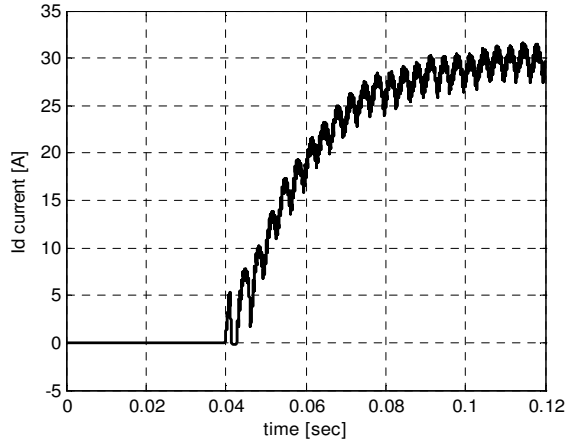

Fig.8. Load current I_d for rectifier mode, $\alpha = 20^\circ$.

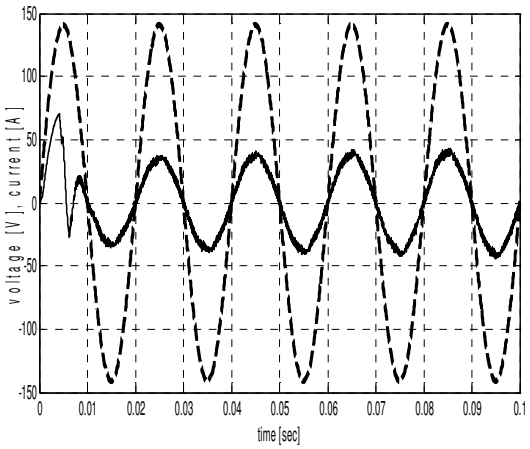

Fig.9. Phase voltage and current for rectifier mode, $\alpha = 20^\circ$.

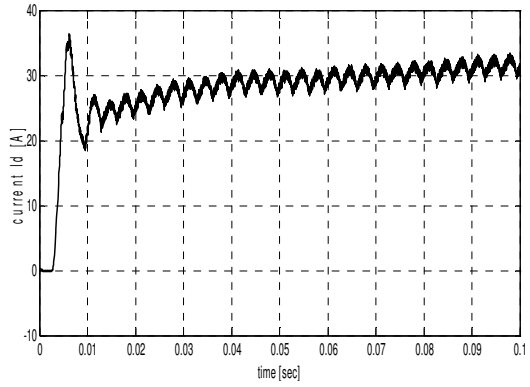

Fig.10. Load current I_d for rectifier mode, $\alpha = 20^\circ$.

In Fig.9 and 10 the same case is presented, but APF and LFCC are connected simultaneously at $t = 0$.

The dynamic of the drawn current, Fig.9, and of the load current, Fig.10, are better, while THD has the same value as above.

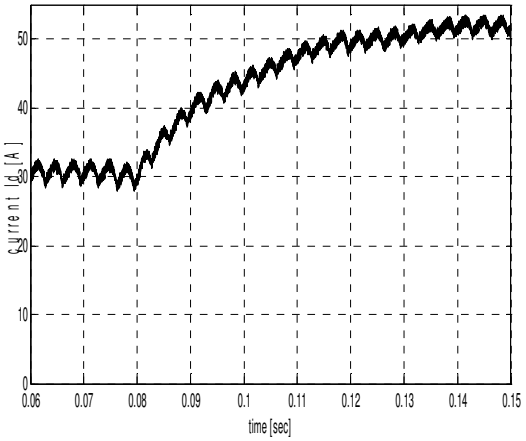

Fig.11. The variation of the load current I_d from 30A to 52A.

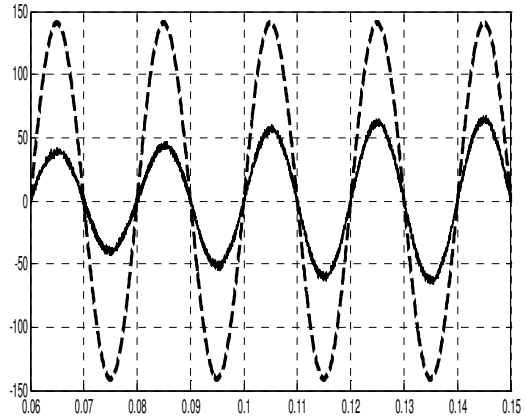

Fig.12. Voltage and drawn current waveforms for the load variation between 30 and 52A.

In Fig.12 the influence of the load current, which is rising from 30 A to 52A at $t = 0.08\sec$, Fig. 11, is presented. The drawn current remains sinusoidal but the THD, calculated in the steady state, diminishes to 3.6%. The diminishing of THD could have the following explanation: the load current having a greater value the accumulated energy in the inductor L_K will be bigger and APF compensation capacity rises.

In Fig.13 and 14 the load current, mains voltage and drawn phase current are plotted, for inverter mode at $\alpha = 150^\circ$ and the load current of 30A. The inverter mode is connected at time $t = 0.04$ seconds, the capacitor C being charged. It can be observed that the phase current and mains voltage are in opposite phase as the power flows from load, D.C. motor, to the mains. After a short time, about half period, the

drawn current becomes near sinusoidal and THD is 8.62%.

The waveforms of the phase voltage and drawn current for a rectifier mode with constant load current and the firing angle changed from 20° to 45° are presented in Figure 15.

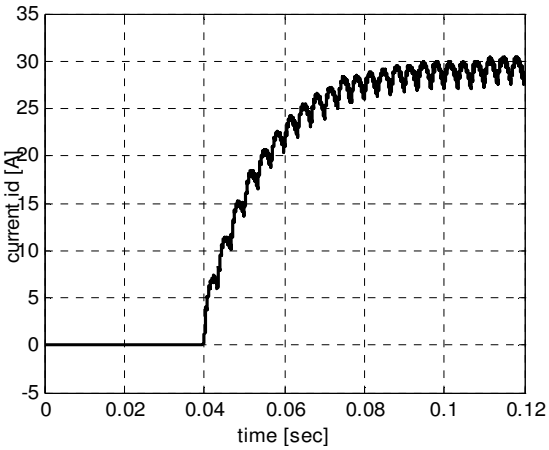

Fig.13. Load current I_d for inverter mode, $\alpha = 150^\circ$.

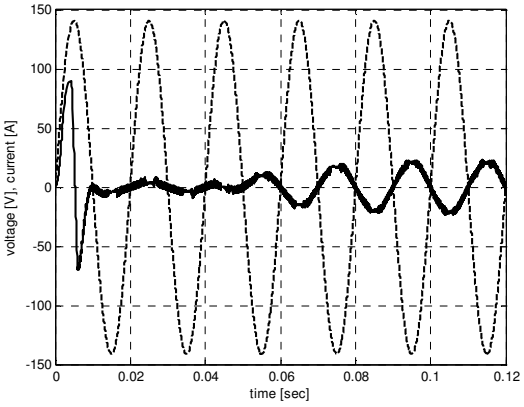

Fig.14. Phase voltage and current for inverter mode $\alpha = 150^\circ$.

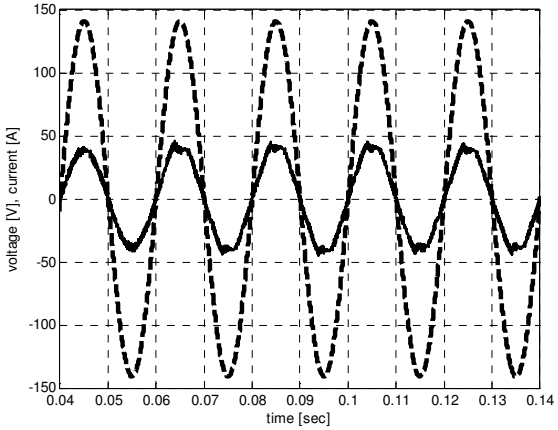

Fig.15. Phase voltage and drawn current for rectifier mode $\alpha = 20^\circ \rightarrow 45^\circ$.

The current, presented in Fig.15, changes little after the time t=0.05, when the firing angle commutation takes place, and THD becomes 6.98%.

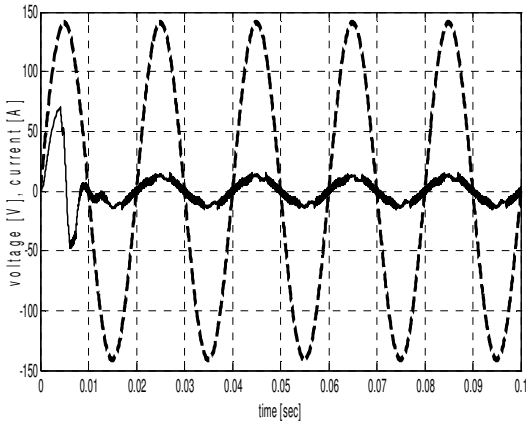

Fig.16. Phase voltage and drawn current for rectifier mode, $\alpha = 70^\circ$ and 5A load current

Another test was made for a firing angle of 70° and a small load current, corresponding to a D.C. motor without restoring torque, when the load current becomes discontinuous. The APF works correctly and THD has the same value as above.

Comparing the initial phases of the mains voltage and current for the all tests it can be concluded that

$$\cos\varphi \cong 1 \quad (21)$$

i.e. the reactive current component is practically complete compensated.

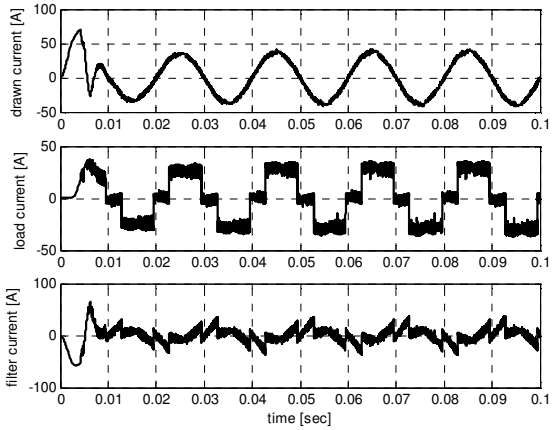

Fig.17. Drawn, load and filter currents.

A very interesting graphic shows the waveform of the three currents, drawn, LFCC and filter, Fig. 17. It can be observed that the filter current has such a form as to respect the equation (16). Also the maximum value of the filter current, except the charging transient regime of the capacitor C, is relatively smaller than LFCC currents, but the switching frequency can be found in the shape of both currents.

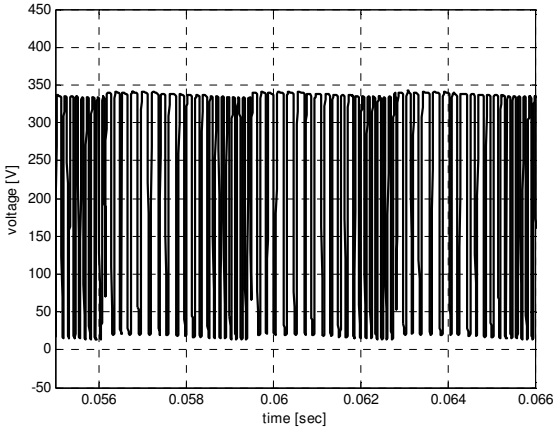

Fig.18. LFCC output voltage.

In Fig.18 three pulses, half supply period, of the LFCC output voltage is presented, for a L_F=0.1mH. The voltage is modulated with APF switching frequency. The L_F inductor assures during switching period a minimum voltage, about 20V, in the aim to avoid the thyristors no conducting and discontinuous current mode. D.C. motor being a R+L load does not influenced by voltage waveform, the current, Fig. 11, having an acceptable ripple. Thee maximum switching frequency, which is determinate by the hysteresis band and L_K inductor was estimated at a value of 7 kHz.

5. CONCLUSIONS

The simulated results prove that the proposed structure is operating accordingly. The substantial decrease of the THD and the unity displacement power factor recommend the solution as a viable option with good performances. The main drawback is the presence of the relatively large inductor L_K. However, this also applies to all the other APF structures. The inductor has to be designed to withstand the currents from the LFCC and also the APF. The solution can be applied to three-phase line-frequency controlled converter having high rating power.

6. REFERENCES

Akagi, H. (1996). New Trends in Active Filters for Power Conditioning, *IEEE Transctions*, IA-32.

El-Habrouk, M., M.K.Darwish and P.Mehta (2000). *Active Power Filters.: A review*, IEE Proc. – Electr. Power Appl, Vol. 147, No. 5, September.

Ionescu, F., S. Nitu, and E. Rosu (2001). *Preocupari actuale in domeniul electronicii de putere*, Editura SECOREX, ISBN 973-85298-3-2, Bucuresti .

Mohan, N., T. Undeland, W. Robbins (2000). *Power Electronics. Converters, Applications, and Design*, Wiley.

Nunez-Zuninga T. E. and J.A. Pomilio (2002) Shunt Active Power Filter Synthesizing Reisitive Loads, *IEEE Transactions in Power Electronics*, **vol.17, No 2**, March.

Rahmani, K.Al-Haddad, F. Fnaiech, and P.Agarwal (2003). Modified PWM with Indirect Current Control Technique Applied to a Single-Phase Shunt Active Power Filter Topology,. IEEE ISIE

Rosu E., M. Culea, M. Nichita, and T. Munteanu (2006). Indirect Control of a Single –phase Active Power Filter, *The Annals of "Dunarea de Jos" University of Galati*, Fascicle III, pp 94-99.